

Binding of 5'-GMP to the GluR2 AMPA Receptor: Insight from Targeted Molecular Dynamics Simulations[†]

Jesús Mendieta,[‡] Federico Gago,[§] and Galo Ramírez*[‡]

Centro de Biología Molecular Severo Ochoa, Universidad Autónoma, E-28049 Cantoblanco, Madrid, Spain, and Departamento de Farmacología, Universidad de Alcalá, E-28871 Alcalá de Henares, Madrid, Spain

Received June 7, 2005; Revised Manuscript Received September 7, 2005

ABSTRACT: Guanine nucleotides behave as competitive antagonists at ionotropic glutamate receptors and show neuroprotective activity in different experimental excitotoxicity paradigms, both in vivo and in cultured cell preparations. Taking 5'-GMP as the reference nucleotide, we have tried to understand how these molecules interact with the agonist-binding site of the GluR2 α -amino-3-hydroxy-5-methyl-4-isoxazolepropionate (AMPA) receptor. Using a crystallographic model of the ligand-binding core of the GluR2 receptor in complex with kainate, we have previously analyzed the structural changes associated to the binding of agonists to the receptor and suggested a mechanism for the coupling of agonist binding to channel gating. In the present investigation we used the structure of the apo form of the receptor to probe the primary interactions between GMP and GluR2 by means of an automated docking program. A targeted molecular dynamics (TMD) simulation procedure was subsequently used to force the closing of the protein and to study the rearrangement of the ligand and surrounding amino acids. The resulting structure provides a plausible model of the nucleotide–receptor complex. Indirect support for the validity of our approach was obtained when the same methodology was shown to yield structures of the kainate–GluR2 and 6,7-dinitroquinoxaline-2,3-dione (DNQX)–GluR2 complexes that were in very good agreement with the published crystallographic structures. Both the stacking interaction between the phenyl ring of Tyr73 and the purine ring of GMP and a salt bridge between the phosphate group of GMP and Arg108 in the S1 domain, together with several hydrogen bonds, are proposed to secure the anchoring of GMP to the agonist-binding site. Unlike conventional competitive antagonists, such as DNQX, occupancy of the site by GMP still allows receptor segments S1 and S2 to close tightly around GMP without interacting with the critical residue Glu209 that triggers channel opening. Thus, GMP appears to be rather a false agonist than a competitive antagonist. This fact and the nature of the energy barriers that stabilize GMP bound to the closed form of the receptor provide an explanation for the unusual behavior of some guanine nucleotides in ligand-displacement experiments.

Excitotoxicity, associated with excessive glutamatergic activity, appears to be a consistent pathogenic factor in many acute and chronic/degenerative disorders of the central nervous system (1). Both abnormally high extracellular glutamate concentrations and alterations in receptor regulation may contribute to the observed toxicity (2–6). The use of glutamate antagonists has then been proposed as a potential therapeutic tool to help to control glutamate receptor hyperactivation (1, 7). Results from binding experiments have consistently shown that guanine nucleotides (GNs)¹ are able to displace receptor-bound glutamate agonists and antagonists (8–11). Pharmacologically, GNs do indeed behave as competitive glutamate antagonists at ionotropic glutamate receptors (iGluRs; 12–16) and display striking neuroprotective activity in different experimental excitotoxicity paradigms, both in vivo and in tissue culture (17–19).

On one hand, in our previous studies (15–19), guanosine 5'-monophosphate (GMP) has been shown to behave as a reliable glutamate antagonist and neuroprotectant, although it is significantly less active than conventional synthetic competitive antagonists and it does not easily cross the blood–brain barrier. On the other hand, GMP is not toxic per se, and it has the additional advantage over GDP, GTP, and their analogues in that it does not interfere with cell-signaling mechanisms involving G-proteins and other GT-Pases. Taken together, these findings support the desirability of designing new nonnucleotidic compounds that interact with ionotropic glutamate receptors in the same way as GMP does.

We have recently used a crystallographic structure of the GluR2 AMPA receptor (20) to analyze the structural changes

[†] Supported by Dirección General de Investigación Científica y Técnica (Grant SAF2003-01721) and by Fundación Ramón Areces.

* To whom correspondence should be addressed. E-mail: gramirez@cbm.uam.es. Telephone: +34-914978449; Fax: +34-914974799.

[‡] Universidad Autónoma.

[§] Universidad de Alcalá.

¹ Abbreviations: AMPA, α -amino-3-hydroxy-5-methyl-4-isoxazolepropionate; CNQX, 6-cyano-7-nitroquinoxaline-2,3-dione; DNQX, 6,7-dinitroquinoxaline-2,3-dione; GDP, 5'-guanosine diphosphate; GluR2, ionotropic glutamate receptor 2; GMP, 5'-guanosine monophosphate; GN, guanine nucleotide; GppNHP, 5'-guanylyl imidodiphosphate; GTP, 5'-guanosine triphosphate; iGluRs, ionotropic glutamate receptors; MD, molecular dynamics; rmsd, root mean square deviation; TMD, targeted molecular dynamics; UMD, unconstrained molecular dynamics.

associated to the binding of agonists to the receptor, and we have proposed a plausible mechanism for the coupling of agonist binding to channel gating (21). We then thought that this model could also be advantageous to predict the structure of the GluR2 receptor when bound to GMP and to identify the critical residues involved in the specific recognition of this nucleotide. However, in the case of receptors such as GluR2, in which the interaction of the ligand takes place, in a first step, with a different conformation of the receptor (generally an "open" form), and then the complex undergoes a conformational change that stabilizes a "closed" form of the ligand–receptor complex, the use of this methodology is not straightforward. We have then resorted to a two-step computational approach that first uses automated docking methods on the open form of the receptor and then is followed by TMD simulations so as to induce the conformational change that leads to the final configuration of the complex. For control purposes, the validity of this approach has been tested on a well-known agonist (kainate) and a typical competitive antagonist (DNQX), each of which forms a distinct complex with the GluR2 ligand-binding core that has been characterized by X-ray crystallography (20, 22). Its subsequent application to GMP has allowed us to propose the structure of GMP-bound GluR2 and to identify putative critical residues involved in the specific recognition of this nucleotide by the receptor. We believe that the information obtained can be of help in the design of nucleotide surrogates that share the low toxicity of GMP, having similar or higher antiexcitotoxic activity, while at the same time being able to reach higher concentrations in brain tissues.

MATERIALS AND METHODS

Experimental Methods

Binding experiments with chick cerebellar membranes were carried out exactly as described previously (23), using [³H]kainate (NEN Life Science NET875, 58 Ci/mmol), [³H]-CNQX (NEN NET1022, 17.27 Ci/mmol), and [³H]GMP (Sigma G5662, 10.4 Ci/mmol) as radioactive ligands and unlabeled kainate, DNQX, and GMP as displacers, at concentrations in the 10⁻⁹ to 10⁻² M range. IC₅₀s were calculated from SigmaPlot 7 built-in logistic equations.

Computational Methods

Docking Studies. A docking exploration with AUTODOCK 3.0 (24) was performed for the three ligands examined. This program allows full flexibility in the ligands, while keeping the geometry of the receptor frozen. The exploration of docking positions was carried out through 100 runs of the Lamarckian genetic algorithm, using the AUTODOCK default parameters. The resulting docking positions were clustered according to an rmsd criterion of 1 Å. The docking exploration was restricted to the region corresponding to the cleft between the two subdomains that make up the ligand-binding core.

Molecular Dynamics Simulations. Molecular dynamics (MD) simulations were performed using the SANDER module of AMBER8 and the parm94 parameter set (25). The open form of the GluR2 receptor that we reported previously (21) was used as input for the MD simulations. An adequate number of Cl⁻ ions were added to neutralize the net positive

charge of the system that includes the protein and the corresponding ligand. The counterions were placed in a shell around the system using a Coulombic potential in a grid. The neutral complex was then immersed in a truncated octahedron solvent box, keeping a distance of 8 Å between the wall of the box and the closest atom of the solute. The counterions and the solvent were added using the LEAP module of AMBER. Initial relaxation of each complex was achieved by performing 10000 steps of energy minimization using a cutoff of 10.0 Å. Subsequently, and to start the MD simulations, the temperature was raised from 0 to 298 K in a 200 ps heating phase, and velocities were reassigned at each new temperature according to a Maxwell–Boltzmann distribution. During this period, the positions of the Cα atoms of the solute were restrained with a force constant of 20 kcal·mol⁻¹·Å⁻¹. In a second phase, lasting 100 ps, the force constant was reduced stepwise. Finally, the system was allowed to relax in the absence of restraints (UMD) for 100 ps. The TMD simulations were then performed by adding an additional penalty term to the energy function:

$$E_i = \frac{1}{2}Kn(R_i - R_0)^2$$

where *K* is the force constant, *n* is the number of atoms used as template, *R_i* is the current rmsd, and *R₀* is the value of the target rmsd. The Cα atoms of the closed form of the S1S2 GluR2 construct (Protein Data Bank code 1GR2) were used as the template. Since TMD, in this implementation, requires a reference structure with exactly the same number of atoms as the system of interest, and the crystal structure lacks two loops (residues 31–45 and 129–143), we have used our previously model-built structure (21) to which we added the counterions and water molecules, in the way explained above, following the replacement of kainate by either DNQX or GMP as required. The target rmsd value was set to 0.0, and the force constant for the TMD was progressively increased (0.05 kcal·mol⁻¹·Å⁻¹ per run) during 10 consecutive runs of 25 ps each. The mean penalty energy was monitored every 25 ps. In the case of the GluR2–GMP complex, two UMD simulations of 1 ns each were performed using as initial conformation either the final structure of the TMD trajectory or an intermediate "snapshot". The SHAKE algorithm was used throughout to constrain all bonds involving hydrogens to their equilibrium values so that an integration time step of 2 fs could be employed. The list of nonbonded pairs was updated every 25 steps, and coordinates were saved every 2 ps. Periodic boundary conditions were applied, and electrostatic interactions were represented using the smooth particle mesh Ewald method with a grid spacing of ~1 Å. Residue numbers referred to in this work correspond to those in the S1S2 GluR2 construct (PDB 1GR2 file).

RESULTS AND DISCUSSION

Experimental Results: Nonreciprocal Displacement of Kainate, CNQX/DNQX, and GMP in Chick Cerebellar Membranes. Some years ago, when carrying out ligand-binding displacement experiments with [³H]kainate and [³H]-GppNHp, in chick cerebellar membranes, we found that while GNs consistently displaced the binding of both ligands in a purely competitive fashion, neither kainate nor glutamate, even at high concentrations, would displace bound [³H]-

Table 1: Cross-Displacement of Kainate, DNQX, and GMP in Chick Cerebellar Membranes^a

tritiated ligand (40 nM)	displacer	IC ₅₀ (M)
kainate	kainate	3.3×10^{-7}
	DNQX	6.0×10^{-7}
	GMP	1.6×10^{-5}
CNQX	kainate	1.7×10^{-7}
	DNQX	1.0×10^{-7}
	GMP	4.8×10^{-5}
GMP	kainate	$> 10^{-2}$
	DNQX	$> 10^{-2}$
	GMP	3.0×10^{-7}

^a Tritiated kainate, CNQX (a close analogue of DNQX), and GMP were displaced with varying concentrations of unlabeled drugs (ranging from 10^{-9} to 10^{-2} M) and the IC₅₀s calculated from the displacement curves by use of SigmaPlot 7 software. Results shown are the mean of two determinations with duplicate samples.

GppNHp (23). Prior to checking whether the computational approach that we have outlined above to explore the interactions between GMP and GluR2 could throw some light on this unexpected behavior, we have repeated the experiments in detail but using [³H]GMP as the tritiated GN and including conventional competitive antagonists in the analysis. Table 1 fully confirms this nonreciprocal displacement pattern that distinguishes GMP from both agonists and proven competitive antagonists. An explanation for this behavior, that takes into account the results of our TMD simulations, is suggested later in this section.

Automated Docking. The open form of the GluR2 ligand-binding core, as previously obtained from a MD trajectory simulating S1–S2 domain separation (21), was used to automatically dock GMP and analyze its interaction with the receptor. Both kainate (a rigid analogue of glutamate with agonistic properties) and DNQX (a typical competitive antagonist), whose binding to the receptor has been structurally characterized (22), were studied in parallel so as to check program performance and establish functional comparisons with GMP.

After 100 docking runs, the results were clustered using a rmsd tolerance of 1.0 Å, and the mean docking energy of each cluster was measured. Figure 1 shows the energy profiles and cluster distributions (only for the first 12 clusters) obtained for kainate, DNQX, and GMP, respectively. In all cases the most populated cluster was also that with the lowest docking energy. It must be noted that, in the open structure, that was used for docking, the binding site is not arranged as in the final conformation of the complex but consists rather of a charged pocket in the S1 domain that the ligand recognizes prior to promoting the closure of the domains (21). An analysis of the docking energy for the structures belonging to the most favorable cluster shows a predominance of the electrostatic term over the van der Waals contributions, which can be explained by the structural considerations described below.

Figure 2 shows the location and orientation of the best solutions for bound kainate, DNQX, and GMP in the GluR2 ligand-binding core. The ligands are placed in the cleft separating the S1 and S2 domains. For all three ligands, most of the contacts are with residues in the S1 domain. The strongest interaction, in all cases, is the salt bridge between the guanidinium group of Arg108 in S1 and the α-carboxylate of kainate, the two keto groups of DNQX, or the

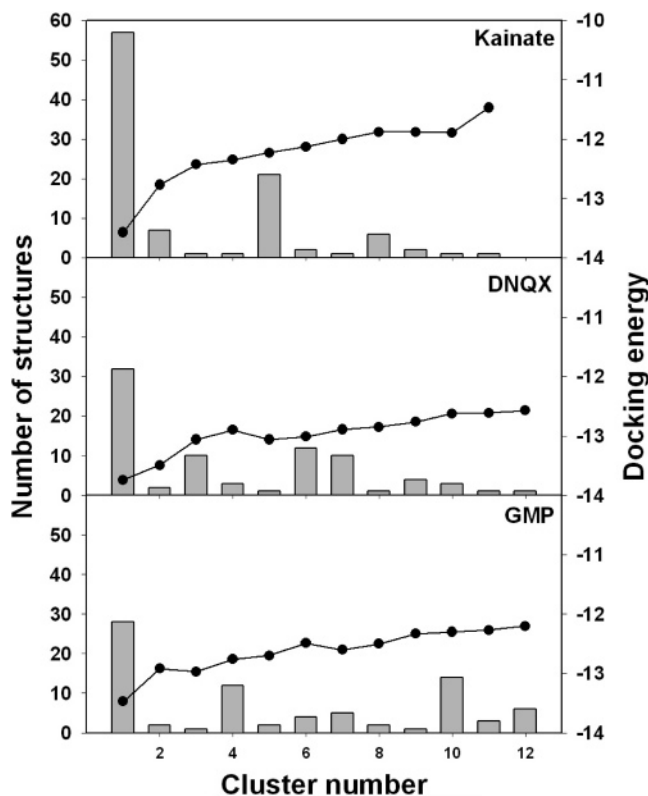


FIGURE 1: Docking of kainate, DNQX, and GMP to the open conformation of GluR2. The resulting structures after docking were clustered according to an rmsd criterion of 1 Å. Bars represent the number of structures included in each cluster. The mean docking energy of each cluster is also shown (●).

phosphate group of GMP, respectively. For both kainate and DNQX this interaction has been described in the X-ray crystal structures of the respective complexes (20, 22). The hydrogen bond observed between the amino group of docked kainate and the amide carbonyl oxygen of Pro101 is also in agreement with the crystallographic structure of the GluR2–kainate complex (20). Ligand recognition by the GluR2 S1 domain through the guanidinium group of Arg108 in an open conformation is consistent with our previous results obtained during the study of the structural changes associated to the binding of agonists to the receptor (21), which suggested that the primary interactions between glutamate or kainate and the open form are established with this domain.

The crystal structure of the GluR2–DNQX complex shows a strong electronic density at the base of helix F (22) that has been attributed to the presence of a sulfate ion, based on its tetrahedral shape and intensity. This anion interacts with the protein mimicking the interactions of the anionic groups of the agonists with helix F. Taking into account the presence of a phosphate group in the GMP, and the homology between the two anions sulfate and phosphate, we have placed a phosphate ion in the GluR2–DNQX complex using the GRID (26) program with a negative probe. Figure 2b shows the phosphate group, after 10000 steps of minimization, in a position close to that found for the sulfate in the crystal structure.

Molecular Dynamics Simulations. To study the behavior of the GluR2 ligand-binding core in the presence of the different ligands, TMD simulations of the three complexes were undertaken. The closing of the domain was forced using the previously adopted closed structure of the GluR2–kainate

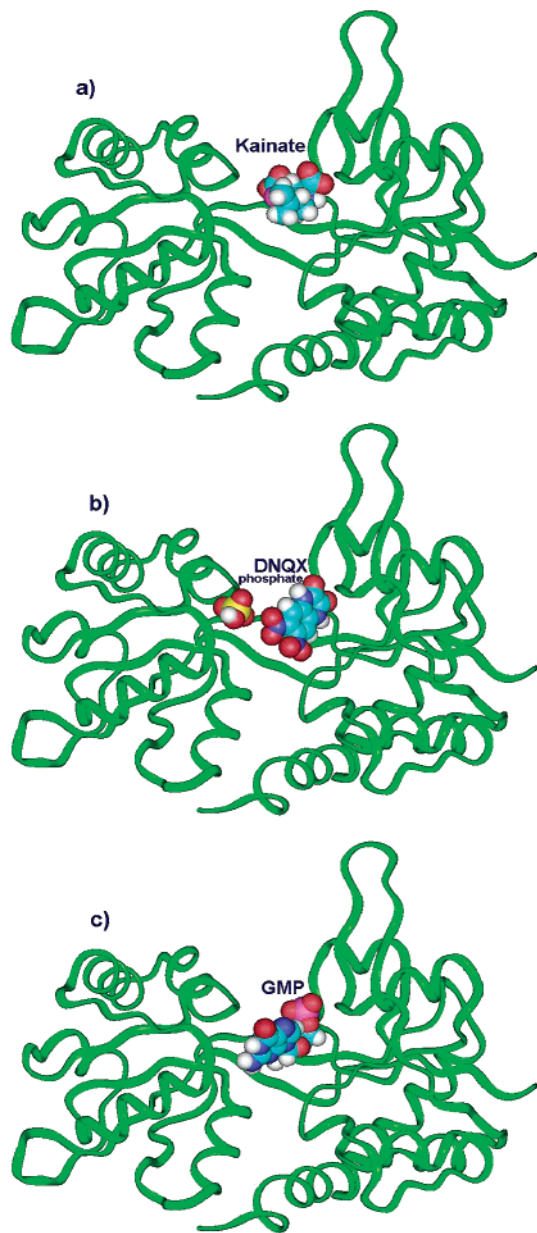


FIGURE 2: Schematic representation of the most favorable docking structure of kainate, DNQX, and GMP in the open conformation of GluR2.

complex as the target (21). The simulations were performed in the presence of explicit water, and no additional restrictions were imposed. Figure 3 shows the degree of domain closure, along the simulation time, monitored as the distance between the C α atoms of residues Ser158 and Arg108, which are located in different domains at the interface and are both involved in kainate binding.

In the case of the kainate complex (Figure 3), closing of the domains happens very rapidly. Before 50 ps the interdomain distance reaches values very close to those found in the three-dimensional structure of the crystallographic kainate–GluR2 ligand-binding core complex. The rmsd between the average structure from the last 100 ps and the crystallographic structure is only 1.4 Å. Most of the interactions that stabilize bound kainate in the closed form can be found in this simulated average structure, including the hydrogen bonds between the 3-carboxymethyl group of kainate, on one side, and the NH groups of Ser158 and Thr159, and the

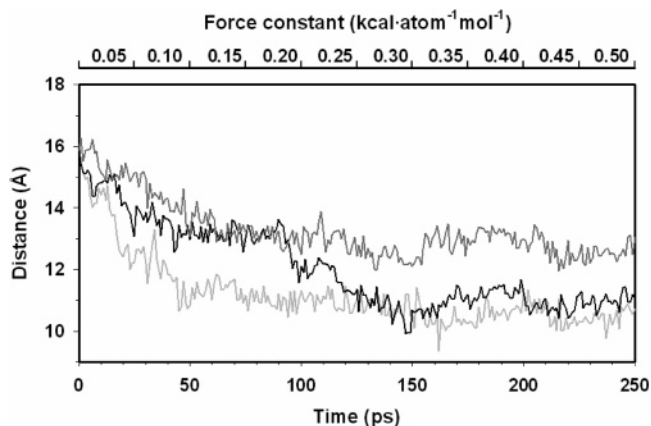


FIGURE 3: Domain closure of GluR2 along the TMD trajectory. Closure was monitored by measuring the distance between C α atoms of residues Arg108 and Ser158. Key: GluR2/kainate (gray), GluR2/DNQX (dark gray), and GluR2/GMP (black).

hydroxyl group of Thr159, on the other side. These two residues are located at the N-terminus of the F helix in the S2 domain. The kainate amino group forms two hydrogen bonds, one with the carboxylate of Glu209 and another with the carbonyl oxygen of Pro101.

In the case of the DNQX complex (Figure 3), closure of the domains is also fast, but the interdomain distance reaches a value of ≈ 13 Å, in good agreement with the 12.0 Å measured in the crystallographic structure of the GluR2–DNQX complex (22) and much higher than that corresponding to the closed form in the presence of kainate (20). The rmsd of the average structure from the last 400 ps of the MD simulation with respect to the crystallographic structure is 2.8 Å, but this relatively high value is mostly a consequence of a different pivoting motion of the S1 and S2 domains with respect to each other, probably as a consequence of the different link used in the construct. In addition to the electrostatic interaction with Arg108 described above, DNQX is stabilized by a stacking interaction between its quinoxalinedione ring and the aromatic ring of Tyr73, as well as by a hydrogen bond between one of the nitro groups and the hydroxyl group of Thr190, both described in the crystallographic complex (22). The position of the phosphate ion incorporated in the initial conformation is placed in a position analogous to that of the sulfate ion in the crystallographic structure. The superpositions of crystal structures of the GluR2, in the presence of kainate and DNQX, and the respective snapshots obtained upon completion of the TMD procedure are shown in Figure 4. The good overall agreement between the simulated and crystallographic structures of the kainate and DNQX complexes supports the validity of this approach.

Domain closure in the presence of GMP shows quite a different behavior (Figure 3). In a first step, the two domains reach a degree of closure similar to that found in the DNQX complex, but after 100 ps, further closing of the domains takes place such that final values similar to those found in the kainate complex are reached and maintained for the rest of the simulation. Even though TMD is not an appropriate method to analyze changes in the energy profile along the conformational transition pathway, we can obtain information about this behavior by monitoring the constraint energy during the TMD simulation (Figure 5). This energy provides

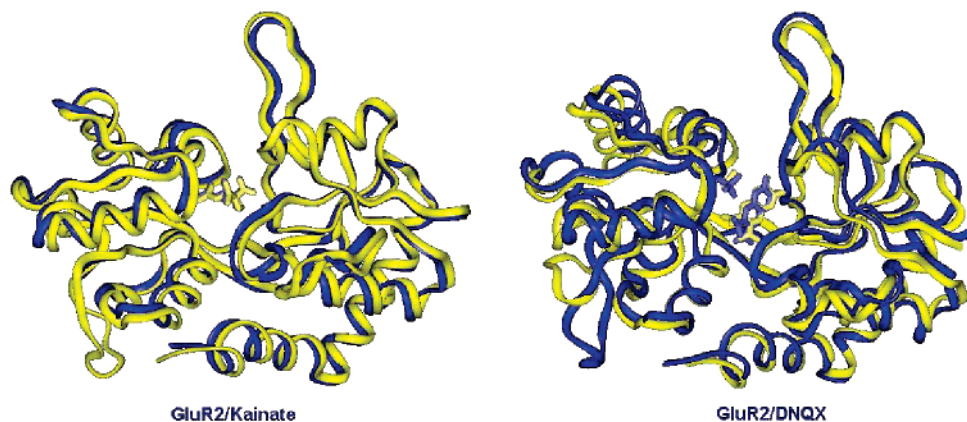


FIGURE 4: Comparison between crystal structures (blue) of GluR2, in the presence of kainate and DNQX, and the snapshots obtained after TMD (yellow).

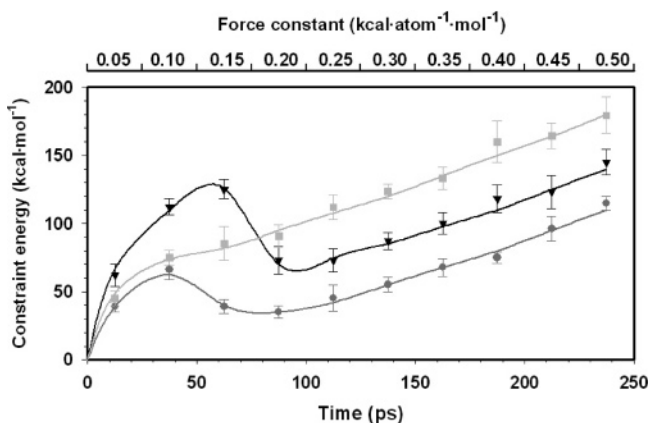


FIGURE 5: Evolution of the constraint energy along the TMD trajectory: GluR2/kainate (circles), GluR2/DNQX (squares), and GluR2/GMP (triangles).

a qualitative estimate of the resistance of the system to adopt the target conformation so that any increments in this value can be interpreted as reflections of the existence of an energy barrier that the system must overcome. Once the energy barrier is surpassed, the system evolves without resistance and the penalty energy decreases. In the case of the GluR2–kainate complex a low energy barrier could be detected between the open and the closed conformations. For force constant values higher than $0.2 \text{ kcal}\cdot\text{atom}^{-1}\cdot\text{mol}^{-1}$ (once the closed conformation has been reached) the energy constraint increased in a linear fashion. In the case of the GluR2–DNQX complex, no local energy minimum could be detected. After a sharp increase, similar to that observed in the case of the GluR2–kainate complex, the constraint energy increased linearly. Interestingly, an energy barrier quite higher than that observed for the GluR2–kainate complex was found during the domain closure motion of GluR2 in the presence of the GMP. This result suggests that the intermediate GluR2 conformation behaves as a transition state and is therefore unstable. To check this possibility, UMD simulations were performed using as starting points the intermediate and the final conformations obtained from the TMD in the presence of GMP (Figure 6). The degree of opening of the GluR2–GMP complex remained constant during the simulation when the simulation started from this final conformation. By contrast, the distance between the two domains increased until it reached values similar to those of the open form when the intermediate conformation was

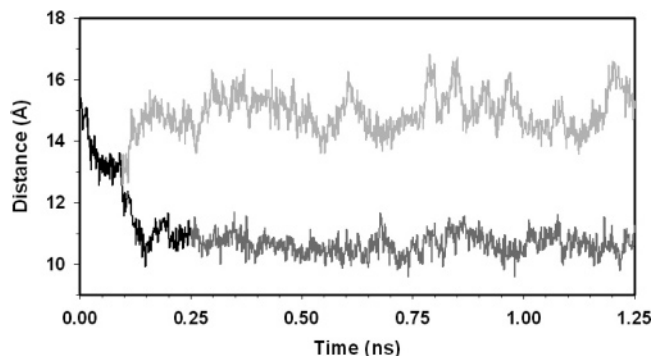


FIGURE 6: Domain closure of GluR2 along the UMD trajectory. UMD was started from the intermediate conformation (gray) and from the final conformation (dark gray) of the TMD trajectory (black). Closure was measured as in Figure 3.

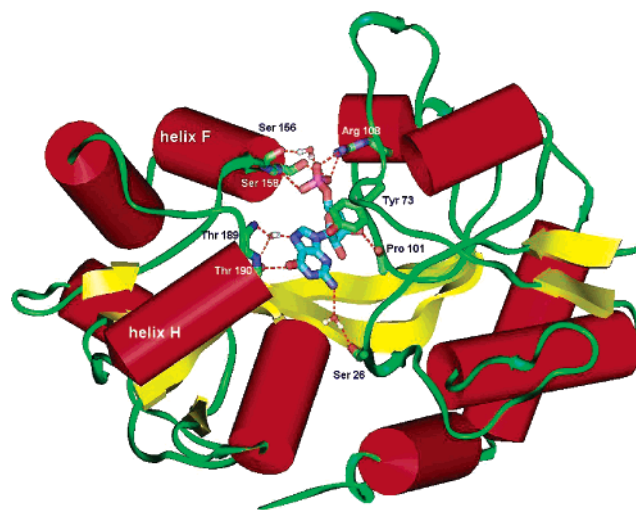


FIGURE 7: Cartoon representation of the proposed structure of the GluR2–GMP complex.

used as the starting point, thus supporting the view that this form is unstable. The stable conformation of the GluR2–GMP complex seems to be the closed form obtained at the end of the TMD procedure.

GMP Binding Site. The GluR2–GMP complex, in its final conformation (Figure 7), is stabilized by several interactions with residues belonging to both the S1 and S2 domains. GMP is almost completely buried in the cleft separating the S1 and S2 domains of the GluR2 ligand-binding core. A stacking interaction with the phenyl ring of the Tyr73 stabilizes the

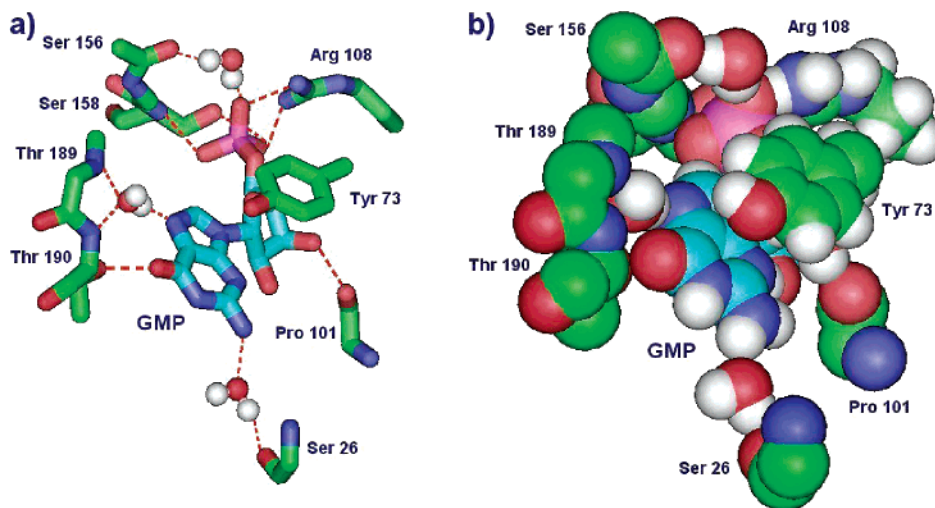


FIGURE 8: Residues involved in GMP binding to GluR2. Hydrogen bonds between GMP and the residues of GluR2 are seen as red dashed lines in the stick representation (a). The van der Waals representation of the atoms (b) is also shown to highlight the stacking interaction between the guanine moiety of GMP and Tyr73.

purine ring of GMP (Figure 8). A similar stacking interaction involving Tyr73 and the quinoxalinedione planar moiety of DNQX has been found in the complex of this antagonist with GluR2 (22).

GMP is also stabilized by hydrogen-bonding interactions involving several residues (Figure 8a). The negative molecular electrostatic potential emanating from the phosphate group allows the formation of a strong salt bridge with Arg108 as well as several hydrogen bonds with polar residues Ser156 and Ser158. As in the case of the kainate complex, these latter interactions take advantage of the macrodipole of the F helix to keep together the S1 and S2 domains. Similar interactions have been found between the N-terminus of the F helix and the sulfate ion present in the crystal structure of the GluR2–DNQX complex (22). The N7 and O6 atoms of guanine (the negatively charged edge of the purine ring) interact with residues Thr189 and Thr190 at the N-terminus of the H helix in a similar way to that of the N-terminus of the F helix. A similar interaction has been described for the 7-nitro moiety of the DNQX and the hydroxyl group of Thr190 (22).

Is GMP a True Antagonist? Unlike what is observed in the complex with the synthetic antagonist, in the complex between GMP and the GluR2 ligand-binding core the degree of closure is similar to that observed in the complexes with agonists. However, GMP has no contact with the carboxylate of the essential Glu209. Formation of a hydrogen bond between the amino group of agonists and the carboxylate of this residue has been previously proposed as the triggering event for channel gating (21). In the closed form of the agonist–GluR2 complexes, this interaction stabilizes the packing of structural elements that connect the ligand-binding core to the first transmembrane segment, which serves as a dynamic link between the ligand-binding event and channel gating. The unpacking of this region in the equally closed form of the GMP–GluR2 complex would allow GMP to behave as a false agonist, and this fact, together with the energy barrier described in Figure 5, would account for the unusual pharmacological behavior of this ligand in binding experiments: whereas the displacement of iGluR agonists and competitive antagonists by GNs is already an established fact (8–11), some years ago we found, to our surprise, that

neither kainate nor glutamate would displace bound [^3H]-GppNHp from chick cerebellar membranes (23). At that time we were at a loss to explain this lack of reciprocity, especially taking into account that GNs behave as pure competitive kainate displacers (23). We have now repeated these experiments with [^3H]GMP, including well-known competitive antagonists in the cross-comparisons, and obtained identical results (Table 1). Interestingly, the behavior of the GMP–(S1S2)GluR2 complex described above offers a simple but plausible explanation for this anomaly. The interaction of kainate and glutamate with the agonist-binding site, and particularly with Glu209, triggers the opening of the ionic channel. In so doing, and as a result of the associated conformational change, the agonist is likely forced to leave this site, which can then be occupied by other ligands in the vicinity, including competitive antagonists and GNs. In contrast, the binding of GMP to the ligand-binding core of GluR2, which does not involve a direct interaction with Glu209 and is further strengthened by the existence of the energy barrier revealed in the TMD experiments, appears to result in a fairly stable complex that is not easily dissociated in the presence of an excess of agonist or competitive antagonist. This false agonist-like nature of GMP fully explains its functional antagonism toward glutamate and other excitotoxic drugs and also its neuroprotective activity. This proposal paves the way for the design of new families of neuroprotective agents based on the molecular scaffold and mode of interaction with iGluRs of the GMP mononucleotide.

CONCLUSIONS

In a substantial number of proteins, including specific receptors, the ligand is buried in a closed-form binding site that is generated during the complex formation. This situation hampers the direct use of structural data from the pharmacological target in the design of active compounds.

In this work we present an approach that circumvents this limitation by using the open structure of the apo form of these receptor proteins to determine the primary interactions between the ligand and the target molecule by automated docking procedures. A subsequent molecular dynamics

simulation under conditions that favor the closing of the ligand-binding cleft and the rearrangement of ligand and surrounding protein residues is used to yield a good approximation to the structure of the closed structure of the complex. The good agreement found between our simulated complexes and those experimentally solved for the kainate–GluR2 and DNQX–GluR2 complexes supports the validity of this approach.

The application of this method to the study of GMP binding to the ligand-binding core of the GluR2 ionotropic glutamate receptor can aid in pointing out the critical residues involved in the specific recognition of this mononucleotide. Furthermore, our simulations have suggested a plausible explanation that accounts for the unusual pharmacological behavior of this ligand. We expect that this information will now be used to design alternative molecular scaffolds that, while sharing the low toxicity of GMP, may be more active and able to achieve higher concentrations in brain tissues.

REFERENCES

- Lipton, S. A., and Rosenberg, P. A. (1994) Excitatory amino acids as a final common pathway for neurologic disorders, *New Engl. J. Med.* **330**, 613–622.
- Olney, J. W. (1978) Neurotoxicity of excitatory amino acids, in *Kainic Acid as a Tool in Neurobiology* (McGeer, E. G., Olney, J. W., and McGeer, P. J., Eds.) pp 95–121, Raven Press, New York.
- Novelli, A., Reilly, J. A., Lysko, P. G., and Henneberry, R. C. (1988) Glutamate becomes neurotoxic via the *N*-methyl-D-aspartate receptor when intracellular energy levels are reduced, *Brain Res.* **451**, 205–212.
- Chen, Q., Olney, J. W., Lukaszewicz, P. D., Almlí, T., and Romano, C. (1998) Ca²⁺-independent excitotoxic neurodegeneration in isolated retina, an intact neural net: A role for Cl⁻ and inhibitory transmitters, *Mol. Pharmacol.* **53**, 564–572.
- Burgos, J. S., Barat, A., and Ramírez, G. (2000) Cl⁻-dependent excitotoxicity is associated with ³H₂O influx in chick embryonic retina, *NeuroReport* **11**, 3779–3782.
- Obrenovitch, T. P., Urenjak, J., Zilkha, E., and Jay, T. M. (2000) Excitotoxicity in neural disorders—the glutamate paradox, *Int. J. Dev. Neurosci.* **18**, 281–287.
- Bräuner-Osborne, H., Egebjerg, J., Nielsen, E. O., Madsen, U., and Krosgaard-Larsen, P. (2000) Ligands for glutamate receptors: design and therapeutic prospects, *J. Med. Chem.* **43**, 2609–2645.
- Monahan, J. B., Hood, W. F., Michel, J., and Compton, R. P. (1988) Effects of guanine nucleotides on *N*-methyl-D-aspartate receptor–ligand interactions, *Mol. Pharmacol.* **34**, 111–116.
- Souza D. O., and Ramírez G. (1991) Effects of guanine nucleotides on kainic acid binding and on adenylate cyclase in chick optic tectum and cerebellum, *J. Mol. Neurosci.* **3**, 39–45.
- Dev, K. K., Roberts, P., and Henley, J. M. (1996) Characterisation of the interaction between guanyl nucleotides and AMPA receptors in rat brain, *Neuropharmacology* **35**, 1583–1593.
- Barnes, J. M., Murphy, P. A., Kirkham, D., and Henley, J. M. (1993). Interaction of guanine nucleotides with [³H]kainate and 6-[³H]cyano-7-nitroquinoline-2,3-dione binding in goldfish brain, *J. Neurochem.* **61**, 1685–1691.
- Baron, B. N., Dudley, M. W., McCarty, D. R., Miller, F. P., Reynolds, I. J., and Schmidt, C. J. (1989) Guanine nucleotides are competitive inhibitors of *N*-methyl-D-aspartate at its receptor site both *in vitro* and *in vivo*, *J. Pharmacol. Exp. Ther.* **250**, 162–169.
- Budson, A. E., Jackson, P. S., and Lipton, S. A. (1991) GDPβS antagonizes whole-cell responses to excitatory amino acids, *Brain Res.* **548**, 346–348.
- Paas, Y., Devillers-Thiéry, A., Changeux, J.-P., Medevielle, F., and Teichberg, V. I. (1996) Identification of an extracellular motif involved in the binding of guanine nucleotides by a glutamate receptor, *EMBO J.* **15**, 1548–1556.
- Burgos, J. S., Barat, A., and Ramírez, G. (2000) Guanine nucleotides block agonist-driven ⁴⁵Ca²⁺ influx in chick embryo retinal explants, *NeuroReport* **11**, 2303–2305.
- Aleu, J., Barat, A., Burgos, J., Solsona, C., Marsal, J., and Ramirez, G. (1999) Guanine nucleotides, including GMP, antagonize kainate responses in *Xenopus* oocytes injected with chick cerebellar membranes, *J. Neurochem.* **72**, 2170–2176.
- Malcon, C., Achaval, M., Komlos, F., Partata, W., Saureissig, M., Ramirez, G., and Souza, D. O. (1997) GMP protects against quinolinic acid-induced loss of NADPH-diaphorase-positive cells in the rat striatum, *Neurosci. Lett.* **225**, 145–148.
- Regner, A., Ramírez, G., Belló-Klein, A., and Souza, D. (1998) Effects of guanine nucleotides on glutamate-induced chemiluminescence in rat hippocampal slices submitted to hypoxia, *Neurochem. Res.* **23**, 523–528.
- Burgos, J. S., Barat, A., Souza, D. O., and Ramírez, G. (1998) Guanine nucleotides protect against kainate toxicity in an *ex vivo* chick retinal preparation, *FEBS Lett.* **430**, 176–180.
- Armstrong, N., Sun, Y., Chen, G.-Q., and Gouaux, E. (1998) Structure of a glutamate-receptor ligand-binding core in complex with kainate, *Nature* **395**, 913–917.
- Mendieta, J., Ramírez, G., and Gago, F. (2001) Molecular dynamics simulations of the conformational changes of the glutamate receptor ligand-binding core in the presence of glutamate and kainate, *Proteins: Struct., Funct., Genet.* **44**, 460–469.
- Armstrong, N., and Gouaux, E. (2000) Mechanisms for activation and antagonism of an AMPA-sensitive glutamate receptor: Crystal structures of the GluR2 ligand-binding core, *Neuron* **28**, 167–181.
- Ramos, M., Souza, D. O., and Ramírez, G. (1997) Specific binding of [³H]GppNHp to extracellular membrane receptors in chick cerebellum: possible involvement of kainic acid receptors, *FEBS Lett.* **406**, 114–118.
- Morris, G. M., Goodsell, D. S., Halliday, R. S., Huey, R., Hart, W. E., Belew, R. K., and Olson, A. J. (1998) Automated docking using a Lamarckian genetics algorithm and an empirical binding free energy function, *J. Comput. Chem.* **19**, 639–1662.
- Case D. A., Plearman, D. A., Cadwell, J. W., Cheatham, T. E., III, Wang, J., Ross, W. S., Simmerling, C. L., Darden, T. A., Merz, K. M., Stanton, R. V., Chen, A. L., Vincent, J. J., Crowley, M., Tsui, V., Gohlke, H., Radmer, R. J., Duan, Y., Pitera, J., Massova, I. Seibel, G. L., Singh, U. C., Weiner, P. K., and Kollman, P. K. (2002) AMBER7, University of California, San Francisco (<http://www.amber.ucsf.edu/amber/amber.html>).
- Goodford, P. J. (1985) A computational procedure for determining energetically favorable binding sites on biologically important macromolecules, *J. Med. Chem.* **28**, 849–857.

BI051084X